

# Damage-Function Analysis of Neutron-Energy and Spectrum Effects Upon the Radiation Embrittlement of Steels

C. Z. SERPAN, JR.

*Metallurgy Division*

and

W. N. McELROY

*Battelle Northwest Laboratory*

July 25, 1969



**NAVAL RESEARCH LABORATORY**  
**Washington, D.C.**



## CONTENTS

|                                     |    |
|-------------------------------------|----|
| Abstract                            | ii |
| Problem Status                      | ii |
| Authorization                       | ii |
| INTRODUCTION                        | 1  |
| EXPERIMENTAL DATA                   | 2  |
| DATA CORRELATION BY DAMAGE FUNCTION | 5  |
| ANALYSIS BY DAMAGE FUNCTION         | 7  |
| DISCUSSION                          | 11 |
| SUMMARY AND CONCLUSIONS             | 12 |
| ACKNOWLEDGMENTS                     | 13 |
| REFERENCES                          | 14 |

## ABSTRACT

Critical evaluations of irradiation effects data for steels exposed in different reactor environments depend upon fluence measurements that reflect the neutron population and the corresponding influence of damage mechanisms inherent to those neutron energy spectra. For the present research investigation, theoretical models describing neutron damage in reactors were adjusted with data on mechanical property changes of A302-B steel irradiated at  $<450^{\circ}\text{F}$  ( $232^{\circ}\text{C}$ ). As described previously, this procedure yielded a damage function that more properly accounts for the energy dependence of damage.

The present investigation was centered on a new comprehensive experiment which yielded wide variations in spectra and in corresponding measurements of neutron embrittlement. The experiment and the resultant data have validated the damage function. An important new part of the damage function analysis technique provides the percent contributions of neutrons of all energy levels to the embrittlement process. Values of the damage function, averaged for a typical reactor physics spectral calculation group structure, are presented with suitable descriptions of their applications to a wide variety of spectra.

One major conclusion reached in this study is that detailed as well as accurate neutron dosimetry measurements of fast and thermal fluxes, corrected to reactor operating temperatures, are necessary if good correlations among irradiation-effects data are to be obtained. This requirement applies to both experimental irradiations and irradiations at reactor component surveillance locations. The study has shown further that an independently derived damage function for irradiation of structural steels such as A302-B at  $<450^{\circ}\text{F}$  ( $232^{\circ}\text{C}$ ) is realistic and can be applied to new experimental data conforming to those conditions. The contributions of thermal and low-energy neutrons to the embrittlement process in low-alloy steel are shown to be of major importance to the interpretation of radiation-effects data.

## PROBLEM STATUS

This is an interim status report. Work on this and other phases of the problem is continuing.

## AUTHORIZATION

NRL Problem M01-14  
RR 007-11-41-5409  
USA-ERG-11-69  
AEC-AT(49-5)-2110

Manuscript submitted April 16, 1969.

# DAMAGE-FUNCTION ANALYSIS OF NEUTRON-ENERGY AND SPECTRUM EFFECTS UPON THE RADIATION EMBRITTLMENT OF STEELS

## INTRODUCTION

The deleterious changes in the mechanical properties of steels caused by the bombardment of neutrons within nuclear reactors become meaningful for immediate application or for projections of future behavior only if the damage-causing fluence of neutrons is well defined. This task is complicated because the neutrons in a flux spectrum create damage by many different mechanisms, all of which must be considered. Because the distribution of neutrons by energy groupings may change drastically for different reactors and reactor locations, it would appear to be impossible to determine a single fluence parameter for best correlation of radiation-effects data. Consequently, techniques have been developed to determine relative damaging effectiveness according to the best available theoretical estimates of the damage process or processes (1-6). Most of these techniques emphasize high-energy neutrons, and one study demonstrated improved correlation by use of damaging fluence  $> 0.5$  MeV (4). The more recent studies of Rossin (5) and Sheely (6) suggest, however, that thermal neutron damage may be significant, since even better correlation of neutron embrittlement in steel vs neutron fluence was attained with the increased importance placed on these neutrons in the respective damage models.

Because the correlation techniques developed so far have not provided for adjustment of the theoretical model by experimental data, a new approach was devised for this purpose (7). This new approach was demonstrated by using ductile-brittle transition temperature increase ( $\Delta TT$ ) data as functions of total neutron fluence, for many irradiations at  $< 450^\circ\text{F}$  ( $232^\circ\text{C}$ ) of ASTM A212-B and A302-B steels in widely differing neutron environments. These data, coupled with their respective neutron spectra, were used to derive a damage function which presented a more realistic weighting of neutron population versus damaging potential for better correlation of experimental data. An additional important use of the damage function was to permit the calculation of total neutron fluence values required to produce a  $200^\circ\text{F}$  ( $111^\circ\text{C}$ )  $\Delta TT$  in A302-B steel in any spectral environment. An advantage of this semiempirical method is that damage caused by mechanisms other than displacement-related processes are included in the damage function.

This report presents the results of a new, comprehensive set of experimental data conforming to the irradiation conditions of the derived damage function (material, temperature, and fluence). The results of this experiment are discussed in terms of their establishing the validity of the damage function. Averaged values of the damage function are tabulated for a typical reactor physics calculation energy group structure, and their application to two different spectra is described. Finally, the damage-function fluences required to cause a  $200^\circ\text{F}$  ( $111^\circ\text{C}$ )  $\Delta TT$  in A302-B steel are presented for many different reactor locations. For each of the spectra involved, the upper and lower energy limits of significantly damaging neutrons are given, and some detail is also provided regarding the contribution of subgroups within the overall energy spectrum.

---

NOTE: This report was the result of a cooperative program between NRL and Battelle Memorial Institute, Pacific Northwest Laboratory, Richland, Washington.

## EXPERIMENTAL DATA

The transition temperature increase data used in this report were measured at the 30 ft-lb (5.2 kgm/cm<sup>2</sup>) level, for a 6-in.-thick (152 mm) plate of A302-B manganese-molybdenum pressure vessel steel. The chemical composition and heat treatment of this plate of steel are shown in Table 1. The irradiations were conducted in a graphite-moderated, water-cooled reactor, designated GMWC. Sealed capsules were contained within special shields that permitted <240°F (116°C) water to pass over the capsules, but which altered the reactor spectrum incident upon the capsules to yield neutron fluence ratios of 1.8, 5, and 9 to 1 thermal to fast (>0.5 MeV). Three distinct fluence levels were attained for each set of capsules, representing all three neutron energy ratios. The  $\Delta TT$  values as functions of fast neutron fluence for the "tailored" GMWC irradiations are depicted in Fig. 1 and summarized in Table 2. (Included in this table for comparison are the A302-B irradiation data used to derive the damage function (7).)

Table 1  
Chemical Composition and Heat Treatment of ASTM Reference  
A302-B Steel Plate 6 in. (152 mm) Thick

| C  | Mn   | P     | S     | Si    | Mo   | Cu   | V       | Al Sol. | N Total |
|--|------|-------|-------|-------|------|------|---------|---------|---------|
| 0.23   | 1.35 | 0.015 | 0.022 | 0.022 | 0.52 | 0.22 | < 0.010 | 0.02    | 0.008   |
| Austenitized at 1650°F (899°C) for 2 hours, water quenched; tempered at 1200°F (649°C) for 6 hours, furnace cooled to below 600°F (316°C). |      |       |       |       |      |      |         |         |         |

The Charpy-V curves of Fig. 1 clearly reveal three distinct levels of  $\Delta TT$  corresponding well to the fluence levels. The specimens exhibited greater-than-average scatter, thus decreasing the overall accuracy of the final  $\Delta TT$  values. The variations in  $\Delta TT$  at the separate levels are, nevertheless, in direct proportion to the fast neutron fluence (>0.5 MeV) taken from Table 2 and do not appear to be caused by the differences in thermal-to-fast (>0.5 MeV) neutron fluence ratios. These results suggest then that thermal-to-fast (>0.5 MeV) neutron populations in the range of ~9:1 for irradiations <450°F (232°C) will have to be exceeded before embrittlement effects of engineering significance can be attributed to thermal neutrons.

The GMWC data have been plotted vs total neutron fluence in Fig. 2; the derivation of the total fluence values is described below. The fluences can be compared in this figure with the  $\Delta TT$  data used to derive the damage function. It is of particular interest to observe that the three data points for each of the three GMWC thermal-to-fast ratios align very well with the arbitrarily placed trend lines superimposed on the figure. The trend pattern is defined as a fourfold increase in total fluence for a 100°F (56°C)  $\Delta TT$  in A302-B steel for irradiations <450°F (232°C). This factor was suggested by Rossin's study (3) and was subsequently used as a reasonable basis for extrapolation of data to other fluence and embrittlement levels (7). Its use is well validated by the results of the GMWC data. Use of the straight-line trend behavior for data  $\leq \Delta TT$  400°F (222°C) is further justified because full radiation embrittlement saturation for this steel irradiated at <450°F (232°C) has not been observed.

The measured iron-wire fluence values >1 MeV in Table 2 are based on a fission-spectrum averaged cross section ( $\bar{\sigma}^{fs}$ ) of 68 millibarns (mb) for the <sup>54</sup>Fe(n,p)<sup>54</sup>Mn reaction; these values are included for reference only. Multigroup neutron spectra were calculated at Battelle-Northwest (4,8) for each position using the diffusion theory code "2DB" (9). Spectra for other reactor locations used in this report were calculated using either the one-dimensional transport theory code "Program S" (10) or the two-dimensional

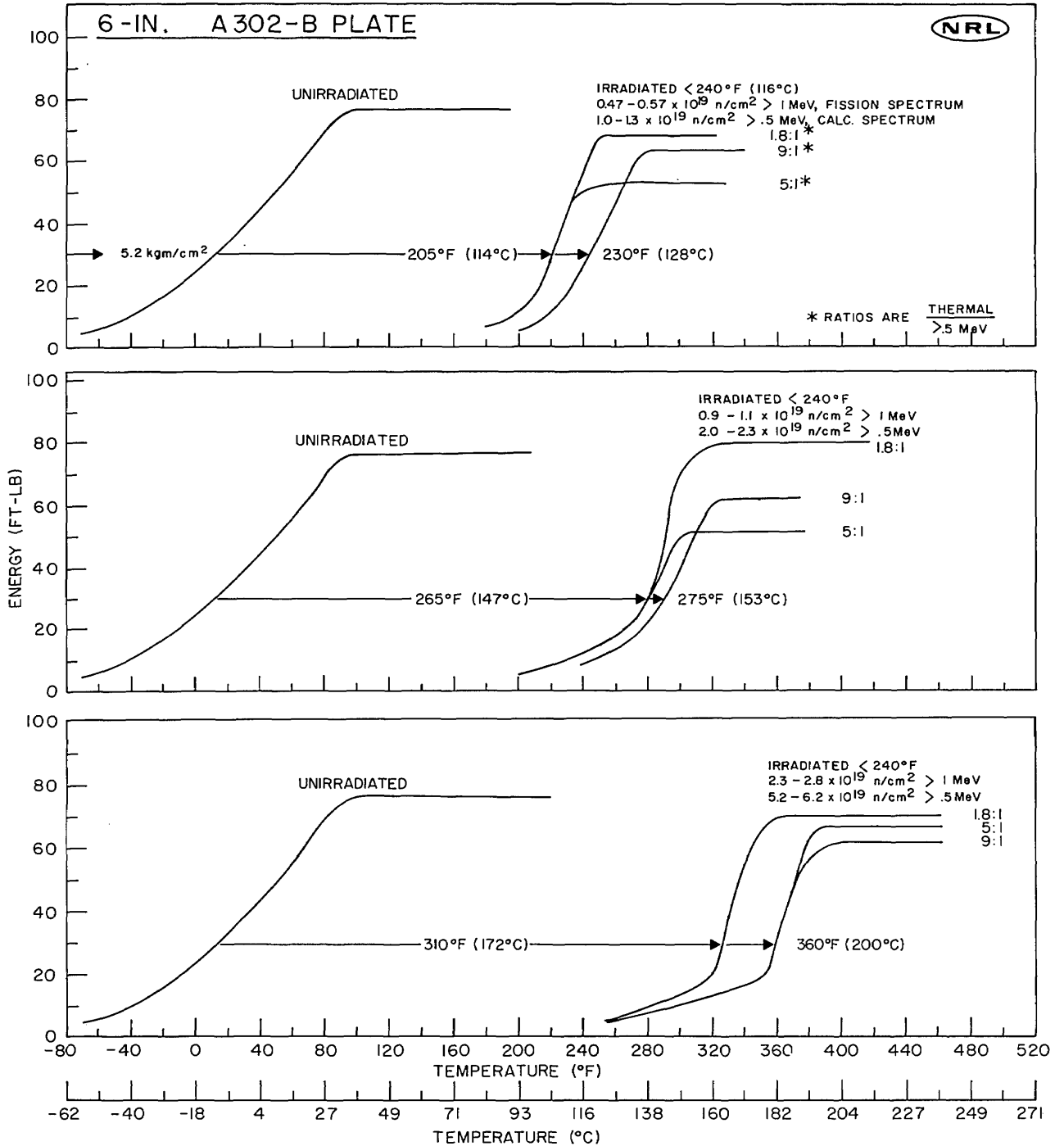


Fig. 1 - Charpy-V notch ductility characteristics of 6-in.-thick (152 mm) A302-B steel before and after irradiation in a graphite-moderated, water-cooled reactor. The neutron spectrum in the reactor location was artificially tailored to yield thermal-to-fast (>0.5 MeV) ratios of 1.8:1, 5:1, and 9:1. The transition temperature increases appear to be in direct relation to the fast (>0.5 MeV) neutron fluence received.

Table 2  
Summary of Transition Temperature Increase and Neutron Fluence Data  
for  $<450^{\circ}\text{F}$  ( $232^{\circ}\text{C}$ ) Irradiations of 6-in.-Thick (152 mm) ASTM A302-B Steel

| Reactor and Facility | Spectrum Reference Number | Charpy-V, 30 ft-lb (5.2 kgm/cm <sup>2</sup> ) Transition Temp. Increase |                    | Measured Neutron Fluence, n/cm <sup>2</sup> (values $\times 10^{19}$ ) |                                       |   |                               |
|----------------------|---------------------------|---|--------------------|--|---------------------------------------|---|-------------------------------|
|                      |                           | $^{\circ}\text{F}$  | $^{\circ}\text{C}$ | >1-MeV Fission Spectrum  | >0.5-MeV Calculated Spectrum          | Thermal Fluence at Mean Reactor Temperature | Total Fluence $>10^{-10}$ MeV |
|                      |                           |   |                    | $\bar{\sigma}^{fs} = 68 \text{ mb}$                                    | $\bar{\sigma}^{fs} = 82.6 \text{ mb}$ |   |                               |
| GMWC* 1.8:1          | 41                        | 205   | 114                | 0.48   | 1.1                                   | 2.0   | 8.3                           |
| 5:1                  | 40                        | 205   | 114                | 0.47   | 1.0                                   | 5.5   | 12.                           |
| 9:1                  | 39                        | 230   | 128                | 0.57   | 1.3                                   | 12.   | 21.                           |
| 1.8:1                | 41                        | 265   | 147                | 0.89   | 2.0                                   | 3.5   | 15.                           |
| 5:1                  | 40                        | 265   | 147                | 0.91   | 2.0                                   | 9.2   | 23.                           |
| 9:1                  | 39                        | 275   | 153                | 1.1  | 2.3                                   | 20.   | 38.                           |
| 1.8:1                | 41                        | 310   | 172                | 2.5  | 5.6                                   | 9.8   | 41.                           |
| 5:1                  | 40                        | 360   | 200                | 2.3  | 5.2                                   | 27.   | 59.                           |
| 9:1                  | 39                        | 360   | 200                | 2.8  | 6.2                                   | 57.   | 101.                          |
| CVTR 10-L            | 1                         | 240   | 133                | 0.78   | 0.80                                  | 124.  | 136.                          |
| HWCTR Gray Rod       | 22                        | 190   | 106                | 0.73   | 0.84                                  | 34.   | 44.                           |
| BGR W-44             | 8                         | 205   | 114                | 0.55   | 1.2                                   | 13.   | 24.                           |
| LITR 18              | 6                         | 255   | 142                | 1.8  | 2.7                                   | 1.9   | 11.                           |
| LITR 28              | 5                         | 220   | 122                | 1.2  | 1.9                                   | 2.1   | 7.2                           |
| LITR 53              | 3                         | 258   | 143                | 1.4  | 2.5                                   | 2.4   | 11.                           |
| LITR 55              | 7                         | 290   | 161                | 2.1  | 3.6                                   | 2.7   | 15.                           |
| LITR 49              | 4                         | 205   | 114                | 0.75   | 1.5                                   | 2.3   | 9.7                           |
| LITR 43              | 21                        | 310   | 172                | 3.1  | 5.0                                   | 3.3   | 19.                           |
| IRL 4-5/8            | 9                         | 105   | 58                 | 0.26   | 0.28                                  | 0.01  | 0.81                          |
| IRL 5-5/8            | 10                        | 80  | 44                 | 0.16   | 0.43                                  | 0.022                                       | 0.62                          |
| IRL 6-5/8            | 11                        | 50  | 28                 | 0.099  | 0.18                                  | 0.0085                                      | 0.51                          |
| IRL 7-5/8            | 12                        | 50  | 28                 | 0.059  | 0.13                                  | 0.0050                                      | 0.40                          |
| IRL 8-5/8            | 13                        | 35  | 19                 | 0.035  | 0.098                                 | 0.0062                                      | 0.32                          |

\* Neutron Spectrum Artificially Tailored. Ratio is Thermal:  $>0.5 \text{ MeV}$

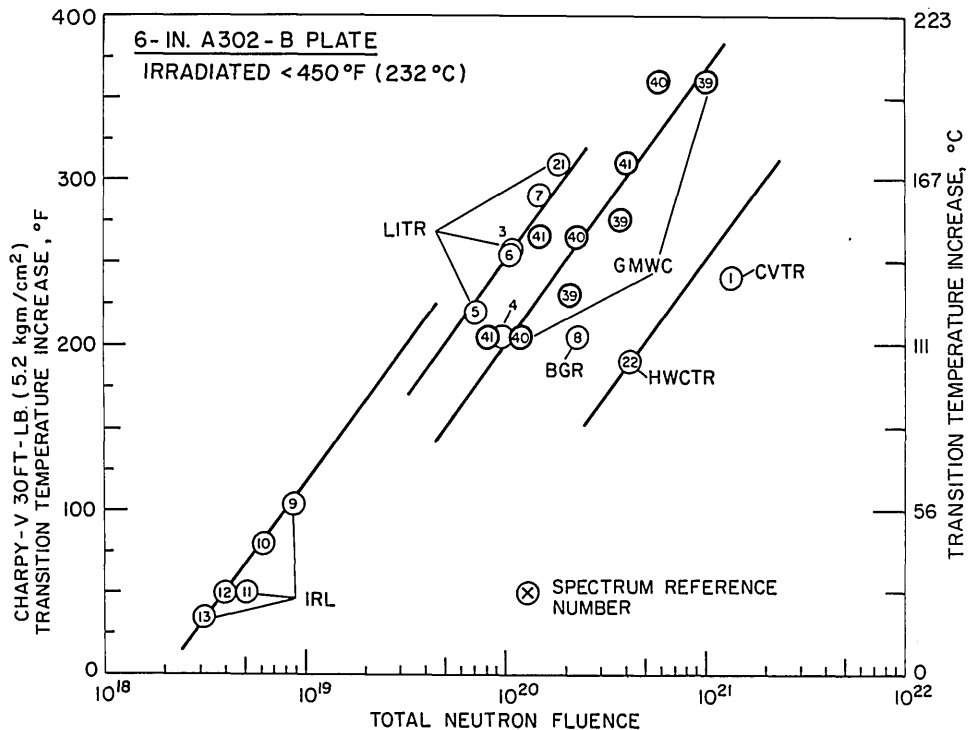


Fig. 2 - Charpy-V 30 ft-lb (5.2 kgm/cm<sup>2</sup>) transition temperature increases vs total neutron fluence for irradiations  $<450^{\circ}\text{F}$  ( $232^{\circ}\text{C}$ ) of A302-B steel. The arbitrarily placed trend lines are used as guides to permit extrapolation of the embrittlement for each numbered spectrum to different levels such as  $200^{\circ}\text{F}$  ( $111^{\circ}\text{C}$ ).

transport theory code "2DXY" (11). The calculated-measured\* fluences  $>0.5$  MeV of Table 2 were based upon  $^{54}\text{Fe}(n,p)$  measurements using an energy-dependent cross section with a  $\bar{\sigma}^{fs}$  of 82.6 mb (12). The use of different  $\bar{\sigma}^{fs}$  values has been discussed (13). For the present study, the thermal fluences were first calculated as 2200 m/sec values from activities measured from the  $1/v$  detector  $^{59}\text{Co}(n,\gamma)$ ; this was accomplished with wires of Al-0.1% Co alloy which were exposed both bare and covered with 0.04 in. (1 mm) of cadmium. These values were then converted to actual thermal fluences by multiplying by  $0.06592(T)^{1/2}$ , where T is an estimated mean reactor temperature in  $^{\circ}\text{K}$  at the location of interest. The actual magnitudes of the thermal ( $\sim 0.4$  eV) and fast ( $\sim 0.5$  MeV) components of each calculated spectrum used in the damage-function analysis procedures were then determined by adjusting the calculated spectrum to agree with the activation detector measurements. The total fluences were then easily derived from the adjusted calculated spectra; the calculated-measured flux  $>0.5$  MeV was divided by the percent flux  $>0.5$  MeV. These total fluences will be referred to as measured values in this report.

#### DATA CORRELATION BY DAMAGE FUNCTION

It can be seen from the ratio of thermal to fast ( $>0.5$  MeV) fluences, Table 2, and from Fig. 2 that the embrittlement in A302-B steel has a neutron energy dependence. From such evidence, it is becoming clear that data obtained from diverse spectral environments can never be completely correlated in a simple plot of  $\Delta\text{TT}$  versus neutron fluence for neutrons greater than any energy. However, for those systems in which  $\geq 90$  percent of the damaging neutrons are predominantly those above a few keV, good correlation can be expected on a plot of  $\Delta\text{TT}$  versus neutron fluence for neutrons greater than a specific energy such as 0.5 or 0.1 MeV (see Refs. 4 and 14). To achieve better correlations, it is necessary to plot the  $\Delta\text{TT}$  data vs another parameter which reflects those mechanisms other than displacements<sup>†</sup> in order to describe the spectral dependency of change (see Refs. 1 through 6). It should be recognized that within the displacement parameter concepts referenced, the measured property changes are not simply plotted vs fluences but vs calculated property changes in the form of displacements. An additional improvement in correlation can be made by use of a damage model that incorporates displacement effects as a starting point and includes provisions to integrate the effects of any other damage or "annealing" (correction) mechanisms. This improved correlation technique still does not permit the direct plotting of measured property changes vs fluences either, but it does allow the comparison of measured vs calculated total fluences for a given amount of neutron embrittlement.

The absolute damage function used to calculate the total fluence required to cause a  $200^{\circ}\text{F}$  ( $111^{\circ}\text{C}$ )  $\Delta\text{TT}$  in A302-B steel for irradiations at temperatures  $<450^{\circ}\text{F}$  ( $232^{\circ}\text{C}$ ) is presented graphically in Fig. 3 (7). A modified version of the SAND-II code (15) was used to obtain the damage function solution  $G(E)$  for a set of integral equations of the form

$$S_j = \iint G(E)\phi_j(E,t)dEdt, \quad (1)$$

where  $S_j$  is a measured integral property change such as  $\Delta\text{TT}$  for a specified material, irradiated for a time  $t$ , in the  $j$ th neutron environment (at constant temperature  $T$ ), and  $\phi_j(E,t)$  is the corresponding  $j$ th neutron differential spectrum.

\*Multigroup spectra results were adjusted in magnitude by the activation detector measurements.

†Displacements are generally thought to be associated with high-energy neutron effects.

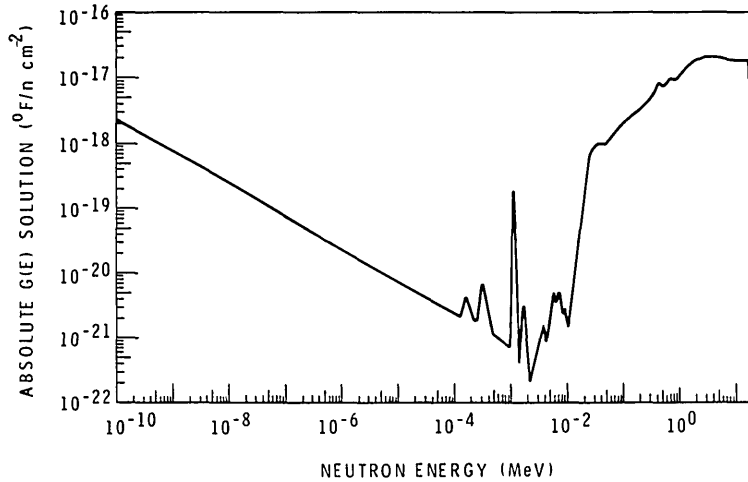


Fig. 3 - Absolute G(E) damage-function solution for a 200° F (111° C) transition temperature increase in A302-B steel for irradiations < 450° F (232° C)

The derived damage function is used with multigroup reactor physics calculations to obtain the fluence (and appropriate energy limits of damaging neutrons) required to cause the property change at the irradiation location of interest. Equation (1) is rewritten:

$$S = \phi t \sum_{i=1}^m G_i \phi_i, \quad (2)$$

where

$$\sum_{i=1}^m \phi_i = 1, \quad (3)$$

$\phi_i$  is the normalized integral flux within the *i*th group,  
 $\phi t$  is the fluence required to cause the 200° F (111° C)  $\Delta TT$ ,  
 $S$  is the property change specified in the derivation of G(E), the damage function,  
 and  
 $G_i$  is the corresponding group-averaged G(E) value.

To use the G(E) function would then require knowledge of the neutron spectrum of the reactor location of interest. Group-averaged values of this (or any) spectrum would be multiplied by group-averaged values of the damage function and Eq. (3) would be solved for  $\phi t$  according to

$$\phi t = S \left[ \sum_{i=1}^m G_i \phi_i \right]^{-1}; \quad (4)$$

the approximate energy limits of damaging neutrons could be inferred by a consideration of each group contribution,  $G_i \phi_i / S \phi t$ , to the total property change. The fluence obtained would be that required to cause a change of  $S$ , in this case a 200° F (111° C)  $\Delta TT$  in A302-B steel, in the spectrum of interest. Fluences for  $\Delta TT$  values other than 200° F can also be calculated (Ref. 7). It was found that a single set of group-averaged values of the damage function (Fig. 3) could be used without introducing more than about a 5-percent variation in the calculated values of fluences for many reactor spectra.

In the development of the damage function of Fig. 3, it was recognized that the reactor environments were not sufficiently different to provide a reliable solution for

the damage model in the intermediate energy region between  $\sim 10^{-7}$  and  $\sim 2 \times 10^{-2}$  MeV. In this region, therefore, the function is essentially a repetition of the assumed input model. For this reason, no attempt was made in this study either to generate or to use detailed structure in this region. Furthermore, for the thermal energy region, the magnitude of the derived damage function for A302-B steel may be too low.

The approximating procedure used in the GMWC experiment (and previously (7)) for defining the magnitudes of thermal, intermediate, and fast components of the neutron spectrum was studied. This approximating procedure has been compared with a more exact procedure based on the SAND-II, multiple-foil activation method (15). This comparison revealed that the approximating procedure may have yielded high thermal fluence results. This implies that the derived damage function may be too low in the thermal energy region. Future reevaluations of these data may reveal, therefore, that the damage from thermal neutrons may be greater than that suggested by the present results.

The foregoing discussion of the limitations of the damage-function analysis technique in no way detracts from the fact that it provides the very best means presently available for correlating radiation effects data from different reactor irradiations. Furthermore, it provides a strong analytical tool for improving the definition of the damaging function of a given spectrum of neutrons. Finally, it provides the only means for satisfactory evaluation of the damaging potential of a neutron spectrum in the absence of measured mechanical property data representative of that spectrum.

#### ANALYSIS BY DAMAGE FUNCTION

Application of Eq. (4) and group-averaged values,  $G_i$ , of the damage function will now be considered in Table 3 using the group integral flux values for two very different reactor irradiation locations. These group-averaged damage-function values are based upon the  $<450^\circ\text{F}$  irradiation behavior of a 6-in.-thick plate of A302-B steel that has been made available to many laboratories in different countries (16). Therefore, these  $G_i$  values could also be used for the analysis of data obtained by other laboratories for irradiations of this steel under the same temperature conditions. Total fluences, using temperature-corrected thermal values, would also have to be used.

In Table 3, the left column under both spectral listings gives the group fluxes as normalized to one neutron, and the middle column is the product of the group flux and the group-averaged damage function. The summation of these products for both spectra are then divided into  $200^\circ\text{F}$  to yield the total fluence for a  $200^\circ\text{F}$   $\Delta\text{TT}$  in A302-B steel for irradiations  $<450^\circ\text{F}$ . The right column under each listing shows the thermal ( $<4.14 \times 10^{-7}$  MeV), intermediate ( $4.14 \times 10^{-7}$  MeV  $< E < 0.183$  MeV), and fast ( $>0.183$  MeV) energy region subtotals for this summation and the corresponding percent contribution to the total damage for these three larger groups. (Note that the total fluences in Table 3 are used to plot the abscissas of the respective data points appearing for these spectra in Fig. 4.)

The GMWC spectrum for the 9:1 thermal-to-fast ( $>0.5$  MeV) ratio was included in Table 3 because it represents the highest such ratio that does not appear to result in more embrittlement than could have been expected for the fast ( $>0.5$  MeV) fluence. It should be clear that the thermal population, even though it be almost an order of magnitude greater than the fast, nevertheless contributes only about 6 percent to the embrittlement. This amount of damage contribution could not be discerned except under the most favorable testing conditions. It is pointed out that the Charpy-V specimen evaluations of the GMWC irradiations revealed more data scatter than may be reasonably expected for this type of steel, and, more specifically, this plate of A302-B steel. On the other hand, three separate data points were developed for each of the fluence ratios in the experiment, and the same behavior pattern of no exceptional embrittlement was observed for every

Table 3  
Group-Averaged Values for Absolute  $G(E)$  for a 200° F (111°C)  $\Delta T$  in A302-B Steel Irradiated at <450° F (232°C) and Application to Different Spectra

| Lower Energy Limit for Group i MeV | Group-Averaged Values $G_i$ ( $^{\circ}\text{F}/\text{n cm}^{-2}$ ) | CVTR   |                        |  | GMWC                   |  |    |  |
|------------------------------------|---|--|------------------------|--|------------------------|--|----|--|
|                                    |   | Spectrum 1 (154:1 Thermal: >.5 MeV)  |                        | Spectrum 39 (9:1 Thermal: >.5 MeV)   |                        | % Contribution by Energy Groups  |    |  |
|                                    |   | $\phi_i$   | $G_i \phi_i$           | $\phi_i$   | $G_i \phi_i$           |  |    |  |
| 7.79                               | $1.81 \times 10^{-17}$  | $4.35 \times 10^{-5}$  | $7.87 \times 10^{-22}$ | $1.29 \times 10^{-4}$  | $2.33 \times 10^{-21}$ | $\frac{101.4 \times 10^{-20}}{119. \times 10^{-20}} \times 100 = 85\%$ |    |  |
| 6.07                               | 1.89  | $1.24 \times 10^{-4}$  | $2.34 \times 10^{-21}$ | 4.76   | 9.00                   |  |    |  |
| 4.72                               | 1.97  | 2.18   | 4.29                   | $1.60 \times 10^{-3}$  | $3.15 \times 10^{-20}$ |  |    |  |
| 3.68                               | 2.07  | 3.36   | 6.96                   | 1.68   | 3.48                   |  |    |  |
| 2.87                               | 2.10  | 5.60   | $1.18 \times 10^{-20}$ | 2.31   | 4.85                   |  |    |  |
| 2.23                               | 1.97  | 7.59   | 1.50                   | 5.10   | $1.00 \times 10^{-19}$ |  |    |  |
| 1.74                               | 1.87  | 7.52   | 1.41                   | 6.54   | 1.22                   |  |    |  |
| 1.35                               | 1.66  | 6.40   | 1.06                   | 8.00   | 1.33                   |  |    |  |
| 1.05                               | 1.33  | 5.85   | $7.78 \times 10^{-21}$ | 8.34   | 1.11                   |  |    |  |
| $8.21 \times 10^{-1}$              | 1.01  | 5.29   | 5.34                   | 8.95   | $9.04 \times 10^{-20}$ |  |    |  |
| 6.39                               | $9.57 \times 10^{-18}$  | 7.01   | $6.71 \times 10^{-21}$ | 9.22   | 8.88                   |  |    |  |
| 4.98                               | 7.95  | 6.28   | 4.99                   | 9.21   | 7.73                   |  |    |  |
| 3.88                               | 8.08  | 4.23   | 3.42                   | 7.48   | 6.04                   |  |    |  |
| 3.02                               | 6.27  | 5.91   | 3.71                   | 8.11   | 5.09                   |  |    |  |
| 2.35                               | 4.47  | 5.85   | 2.62                   | 7.68   | 3.43                   |  |    |  |
| 1.83                               | 3.47  | 7.03   | 2.44                   | 6.74   | 2.34                   |  |    |  |
|                                    |   | $\sum_{i=1}^{16} G_i \phi_i = 1.03 \times 10^{-19}$  |                        | $\sum_{i=1}^{16} G_i \phi_i = 101.4 \times 10^{-20}$   |                        |  |    |  |
| $4.14 \times 10^{-7}$              | $3.0 \times 10^{-19}$   | $8.03 \times 10^{-2}$  | $0.24 \times 10^{-19}$ | $3.48 \times 10^{-1}$  | $10.4 \times 10^{-20}$ |  | 9% |  |
| $1.00 \times 10^{-10}$             | $1.32 \times 10^{-19}$  | $9.11 \times 10^{-1}$  | $1.20 \times 10^{-19}$ | $5.60 \times 10^{-1}$  | $7.39 \times 10^{-20}$ |  | 6% |  |
|                                    |   | $\sum_{i=1}^{18} G_i \phi_i = 2.47 \times 10^{-19}$  |                        | $\sum_{i=1}^{18} G_i \phi_i = 119. \times 10^{-20}$  |                        |  |    |  |
|                                    |   | $\phi t = \frac{200^{\circ}\text{F}}{2.47 \times 10^{-19}} = 8.10 \times 10^{20} \text{ n/cm}^2$ |                        | $\phi t = \frac{200^{\circ}\text{F}}{119. \times 10^{-20}} = 1.68 \times 10^{20} \text{ n/cm}^2$ |                        |  |    |  |

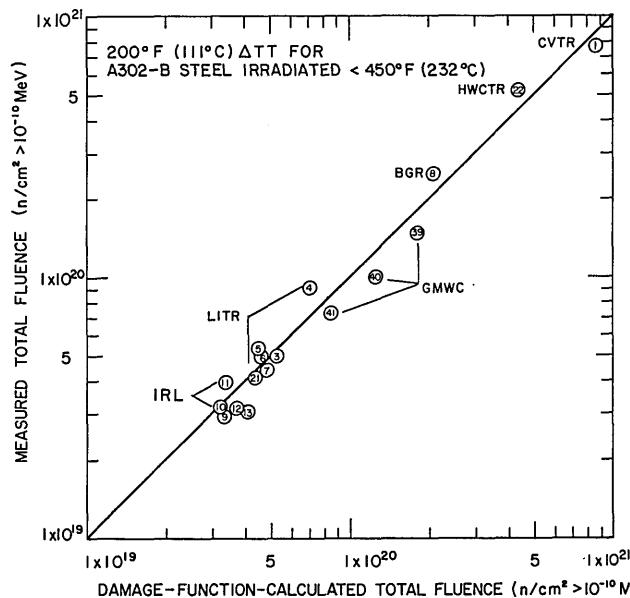


Fig. 4 - Verification of the G(E) damage function by the graphite-moderated, water-cooled reactor (GMWC) irradiation data. The damage-function-calculated fluence agrees very closely with the measured fluence for a 200°F (111°C) transition temperature increase in A302-B steel.

fluence and fluence ratio condition. When the techniques employed in this paper for evaluating and reporting all the fluence values are used, then a thermal-to-fast neutron ratio in the range of 9:1, as displayed by the GMWC data, does not appear to contribute increased embrittlement in A302-B steel for irradiations <450°F.

The spectrum from the heavy-water-moderated CVTR (Carolinas-Virginia Tube Reactor) was selected for Table 3 because it demonstrates exceptionally high thermal-to-fast (>0.5 MeV) fluences. A ratio of 154:1 was measured at the irradiation location. The result of the irradiation was evidence of more embrittlement than would have been expected on the basis of the fast neutron fluence alone. Inspection of the damage percent contributions by energy ranges clearly reveals that thermal and intermediate energy range neutrons are responsible for over half of the embrittlement. The damage contribution percentages of Table 3 provide a means for understanding the increased embrittlement of the CVTR data, relative to that from a GMWC irradiation, which could not be gained simply from the embrittlement-vs fluence values alone.

The critical question of this investigation was to determine whether the damage function is applicable to the GMWC data. The means employed to effect this comparison was to determine from Fig. 2 the measured total fluences to cause a 200°F  $\Delta$ TT in A302-B steel for all three GMWC spectra and plot them vs total fluence values determined by the damage-function-calculated process shown in Table 4. The measured and damage-function-calculated total fluences are compared in Fig. 4. Perfect correlation is achieved when all points fall on the solid line; that is, the damage function can be used to calculate total fluences that agree exactly with measured fluence values for any reactor environment. The average value of ratios of measured to calculated fluences, Fig. 4, have a 15.2-percent standard deviation about a line representing perfect correlation. It can be seen that the GMWC data points (spectra 39, 40, and 41) compare favorably with that amount of deviation. This indicates that the damage function, considering the limitations previously

Table 4  
Prediction of Fluence and Energy Response Necessary to Produce a 200°F (111°C) ΔTT in A302-B Steel

| REACTOR POSITION          | FLUENCE<br>$n/cm^2 \times 10^{19}$<br>$> 10^{-10} MeV$ | 90% DAMAGE ENERGY LIMITS, MeV |             | DAMAGE CONTRIBUTION FROM SPECIFIC ENERGY GROUPS, % |   |                            |
|---------------------------|--|-------------------------------|-------------|--|---|----------------------------|
|                           |  | $E_{lower}$                   | $E_{upper}$ | $E < 4.14 \times 10^{-7}$ MeV                      | Intermediate<br>MeV<br>$4 \times 10^{-7} < E < 0.183$ | Fast<br>$E < 0.183$<br>MeV |
| GMWC1:8:1 T: > .5         | 8.3  | $9.6 \times 10^{-2}$          | 4.4         | 1.   | 7   | 92.                        |
| GMWC 5:1 T: > .5          | 12.  | $5.8 \times 10^{-2}$          | 4.3         | 3.   | 8.  | 89.                        |
| GMWC 9:1 T: > .5          | 17   | $2.2 \times 10^{-1}$          | 4.3         | 6.   | 9.  | 85.                        |
| CVTR 10-L                 | 81   | $7.2 \times 10^{-2}$          | 4.0         | 51.  | 5.  | 44.                        |
| HWCTR GRAY ROD            | 42.  | $1.5 \times 10^{-2}$          | 5.0         | 21.  | 10.   | 69.                        |
| LITR 53                   | 5.2  | $1.7 \times 10^{-1}$          | 4.8         | 0.7  | 5.3   | 94.                        |
| LITR 18                   | 4.6  | $1.9 \times 10^{-1}$          | 4.9         | 0.5  | 4.5   | 95.                        |
| BGR W-44                  | 21.  | $4.5 \times 10^{-2}$          | 4.0         | 7.5  | 8.5   | 84.                        |
| IRL 4 5/8-IN. IN BLOCK    | 3.   | $2.6 \times 10^{-1}$          | 5.7         | 0.3  | 3.7   | 96.                        |
| IRL 6 5/8-IN. IN BLOCK    | 3.4  | $1.8 \times 10^{-1}$          | 4.9         | 0.03   | 6.  | 94.                        |
| IRL 8 5/8-IN. IN BLOCK    | 4.0  | $1.4 \times 10^{-1}$          | 3.7         | 0.04   | 7.  | 93.                        |
| YANKEE ACCEL. SURV.       | 17.  | $3.4 \times 10^{-2}$          | 6.1         | 9.   | 3.  | 88.                        |
| YANKEE V. WALL. SURV.     | 7.1  | $1.4 \times 10^{-1}$          | 6.7         | 2.5  | 2.5   | 95.                        |
| YANKEE PWV / SSCladd      | 5.2  | $2.1 \times 10^{-1}$          | 6.7         | 1.   | 4.  | 95.                        |
| PM-2A PWV / SSCladd       | 9.0  | $7.6 \times 10^{-2}$          | 6.3         | 4.   | 4.  | 92.                        |
| PM-2A 1/4 Thickness       | 6.3  | $1.4 \times 10^{-1}$          | 6.3         | 3.   | 4.  | 93.                        |
| PM-2A 3/4 Thickness       | 3.8  | $2.2 \times 10^{-1}$          | 6.2         | 1.   | 5.  | 94.                        |
| BRP ACCEL.SURV.           | 18.  | $3.0 \times 10^{-2}$          | 6.0         | 10.  | 5.  | 85.                        |
| BRP V. WALL. SURV.        | 10.  | $2.6 \times 10^{-1}$          | 6.6         | 5.   | 5.  | 90.                        |
| BRP PWV / SSCladd         | 7.6  | $1.0 \times 10^{-1}$          | 6.4         | 3.   | 5.  | 92.                        |
| BRP 1-IN. IN WALL         | 6.6  | $1.1 \times 10^{-1}$          | 6.2         | 3.   | 6.  | 91.                        |
| BRP 3-IN. IN WALL         | 5.7  | $1.1 \times 10^{-1}$          | 5.7         | 2.   | 7.  | 91.                        |
| BRP 5-IN. IN WALL         | 5.6  | $1.1 \times 10^{-1}$          | 5.2         | 1.5  | 8.5   | 90.                        |
| OMRE P.V. WALL            | 3.6  | $2.6 \times 10^{-1}$          | 5.3         | 1.5  | 3.5   | 95.                        |
| OMRE CORE CENTER          | 5.6  | $2.0 \times 10^{-1}$          | 5.9         | 0.4  | 3.6   | 96.                        |
| SM-1A PWV / SSCladd       | 6.4  | $1.6 \times 10^{-1}$          | 6.0         | 0.5  | 5.5   | 94.                        |
| EBR-II 2.5cm from center  | 2.3  | $1.9 \times 10^{-1}$          | 4.5         | -  | 6.  | 94.                        |
| EBR-II 77.1cm from center | 5.5  | $6.9 \times 10^{-2}$          | 1.2         | -  | 26.   | 74.                        |
| CP-5 FUEL                 | 6.8  | $1.3 \times 10^{-1}$          | 5.0         | 0.3  | 6.7   | 93.                        |
| CP-5 DUMMY                | 19.  | $1.1 \times 10^{-2}$          | 5.1         | 4.6  | 14.   | 82.                        |

KEY TO REACTORS IN TABLE 4

- BGR Brookhaven Graphite Reactor
- BRP Big Rock Point Reactor
- CP-5 Chicago Pile No. 5, heavy-water test reactor at Argonne National Laboratory. Fuel, within hollow center of fuel-bearing element; Dummy, within hollow center of non-fuel-bearing element.
- CVTR Carolinas-Virginia Tube Reactor, position 10-L
- EBR-II Experimental Breeder Reactor II
- GMWC Graphite-Modulated, Water-Cooled Reactor
- HWCTR Heavy-Water Components Test Reactor, irradiation location in "gray" control rod
- IRL Industrial Reactor Laboratory, Inc. 4-5/8 in. from core face
- LITR Low-Intensity Test Reactor, core lattice position 53, 18
- OMRE Organic Moderated Reactor Experiment, inner edge of pressure vessel wall
- PM-2A Army portable power reactor, Camp Century, Greenland; 1/4, 3/4 thicknesses are locations inside the steel pressure vessel wall.
- SM-1A Army stationary power reactor, Ft. Greely, Alaska

indicated, is applicable to the GMWC spectral shapes for the characteristic embrittlement created within them and for the temperature-material conditions.

## DISCUSSION

If the damage-function analysis technique is to be useful, it should permit the projection of the fluence required in a new spectrum to create a given amount of radiation damage and the percent contributions of neutrons in different energy regions. These damage functions should also permit the prediction of the amount of damage for a stated amount of fluence, provided these are within the validated limits (materials, temperature, and fluence) of the damage function. Using the damage function of Fig. 3, a large number of different neutron spectra were analyzed by computer to determine the total fluence required to produce a 200°F  $\Delta$ TT in A302-B steel if it could be irradiated at <450°F in the facility. The results of this analysis are presented in Table 4.

The energy limits corresponding to the neutrons responsible for causing 90 percent of the radiation embrittlement are tabulated and presented graphically in the table. The total fluence is presented as well as the percent contribution to damage by neutron energy regions. If correlations sufficiently accurate for engineering applications are to be achieved for reactor environments as diverse as shown here, it should be clear that accounting for neutrons of energies greater than 1 MeV or even 0.5 MeV will not be adequate. Further consideration of the graphical portion of Table 4, however, reveals that a threshold of about 0.1 MeV could be used with a reasonable degree of effectiveness for correlations between many reactor environments. The danger inherent in universal employment of the ">1 MeV" concept for data correlation among diverse reactor environments, however, is demonstrated by the energy response range of the "EBR-II 77.1 cm from center" data. This location is in the blanket of the Experimental Breeder Reactor. In the upper limit for 90-percent damaging neutrons is 1.2 MeV based upon the damage function of Fig. 3. To account for  $n/cm^2 > 1$  MeV for this reactor location would be to ignore more than 90 percent of the neutrons effective in causing radiation damage by mechanisms effective in causing <450°F embrittlement in low-alloy steels.

Other data are included in Table 4 for interest, although the application of the <450°F damage function is hypothetical. This is because the operating temperatures of these reactors are in excess of 450°F and thus permit simultaneous irradiation and annealing. The Yankee and Big Rock Point (BRP) relate to pressurized and boiling-water power reactors, respectively. The PM-2A and SM-1A are relatively compact, light-water reactors used by the U.S. Army for electrical power production at remote locations. The OMRE is the now-decommissioned Organic Moderated Reactor Experiment, and the CP-5 is a heavy-water-moderated and -cooled test reactor. In every case in which a large percentage of the damage is attributed to thermal neutrons, a relatively high ratio of thermal to fast neutrons exists.

As noted previously, increased radiation damage apparently can be caused by high populations of thermal neutrons relative to fast (>0.5 MeV) when the ratio exceeds the range of ~9:1, i.e., the GMWC data did not appear to show increased damage, but the 11.2:1 ratio of the BGR did appear to do so (14). On the other hand, the pressure-vessel wall locations of light-water power reactors operating at temperatures >450°F appear to have ratios less than ~9:1 but, nevertheless, seem to be associated with increased radiation embrittlement (13,17). At present, no satisfactory explanation is known for this apparent anomaly. At elevated temperatures, however, there may be a significant reduction in displacement-related damage due to annealing effects. Accordingly, it may be postulated for elevated temperature tests that nondisplacement, low-energy neutron damage would provide a larger relative contribution to the total damage. This then suggests a possible explanation of the apparent power reactor embrittlement anomaly.

The integral effect of all the damage mechanisms occurring in the embrittlement of low-alloy steel at irradiations  $< 450^{\circ}\text{F}$  is exhibited by the differences in total fluences shown in Table 4. The exceptionally wide range of total fluences suggests that it may indeed be impossible to ever formulate a correlation technique based on an approach wherein the neutrons of energies greater than some threshold such as 1 MeV are simply totaled by numbers with no accounting for their differing damage potential. This type of correlation would depict a single-trend, line behavior of increasing radiation damage for increasing total neutron fluence values regardless of the reactor environment. This type of trend behavior can only be used for carefully selected reactors wherein the spectral characteristics are quite similar. For reactors of significantly diverse spectral characteristics, such as in-core locations of light-water test reactors and vessel wall locations of light-water power reactors, it cannot be used.

## SUMMARY AND CONCLUSIONS

This study has demonstrated the applicability of a damage function to the neutron embrittlement and related total fluence of three different neutron spectra. This damage function was developed to calculate the total fluence required in a given spectrum to cause a  $200^{\circ}\text{F}$  transition temperature increase at the Charpy-V, 30 ft-lb level in A302-B steel for irradiations at  $< 450^{\circ}\text{F}$ . The three GMWC spectra used to test the damage function were within the extremes of ratios of thermal to fast ( $> 0.5$  MeV) neutrons used for the function development but are, nevertheless, significant because they cover the most reasonable range of neutrons in many test and power reactors. The good agreement between damage-function-calculated fluences and the measured fluences from the new experimental data establishes the damage-function technique as being valid for its intended purpose.

Group-averaged values for the damage function in terms of a typical reactor physics spectral calculation group structure are presented for use in analyzing  $< 450^{\circ}\text{F}$  irradiation data for an ASTM A302-B steel plate, and the techniques are presented and described. Several cautions are noted, however, regarding the immediate use of the damage function. Most importantly, the total fluence must be used. For this study, foil measurements of iron, for fast neutron determinations, and bare plus cadmium-covered cobalt foils were used to define the thermal fluence. The thermal fluence was further adjusted for the mean reactor operating temperature. These foil measurements were then used to adjust the magnitude of the detailed reactor physics spectral calculations of the irradiation locations. On completion of the analysis discussed in this report, the neutron spectra for the GMWC experiments presented were reevaluated with the SAND-II code and the saturated activities of the iron and cobalt foils. The results strongly suggest that the thermal flux components may have been significantly overestimated. If this is the case, then the 9:1 ratio of thermal to fast ( $> 0.5$  MeV) neutrons would not be a realistic upper limit for the absence of neutron embrittlement in excess of what could be expected from just the fast neutron fluence alone. The more accurate ratio would be a lower value.

The application of the damage function to neutron spectra from which there are no corroborating mechanical property measurements was also presented. Certain of these cases were hypothetical because it would have been difficult to effect irradiations at  $< 450^{\circ}\text{F}$  in reactors whose operating temperatures were  $100^{\circ}\text{F}$  ( $56^{\circ}\text{C}$ ) above this level. These results dramatically revealed the need to account for all neutrons in many, if not most, reactor locations considered, if good correlations or predictions of data are to be made. This analysis also provided a fluence for a  $200^{\circ}\text{F}$   $\Delta\text{TT}$  in A302-B steel in these reactors, thereby providing a means to utilize the comparison of measured and calculated fluence values of Fig. 4. This comparison graphically displays the damaging potential of the spectrum in relation to other spectra. The potential of such comparisons is considerable if one considers that designers planning new reactors can simply test the spectrum calculated for their new reactor with the damage function and immediately

know if the type of radiation damage they desire (for a test reactor) or do not desire (for a power reactor) will be present. If the damage function results suggest undesirable neutron embrittlement conditions, then changes can be made at the design stage, a new spectrum calculated for the modified reactor configuration, and the embrittlement conditions reevaluated with the damage function. The process can be repeated if necessary until the desired reactor conditions are achieved. Thus, it need not be necessary to construct a reactor before a realistic assessment of its potential for radiation damage can be made.

A final conclusion of this study is that detailed and accurate neutron dosimetry measurements are necessary if good correlations of irradiation effects data are to be obtained. It should be clear that good detail in spectral calculations and foil measurements is required for both low- and high-energy neutrons. The use of iron and cobalt foils without a spectral calculation will be inadequate. If a good spectral calculation is available, however, then iron and cobalt foils can be successfully used to define the magnitude of the spectral shape. If such a calculation is not available, then a suitable energy spectrum may be derived from the analysis of a number of different flux-detector foils with overlapping energy-response ranges. Experimenters and designers of pressure-vessel surveillance programs should be sure to provide for the exposure of both high- and low-energy neutron foils, such as iron and both bare and cadmium-covered cobalt foils, within irradiation experiments and at structural component surveillance locations. The availability of these data will be of significant value to the subsequent analysis of the data and will permit far more accurate assessments of the present component condition as well as permit better predictions of future conditions.

#### ACKNOWLEDGMENTS

This research was conducted at the Naval Research Laboratory under the sponsorship of the Office of Naval Research and of the U.S. Atomic Energy Commission under contract AEC-AT(49-5)-2110; the research at the Battelle Memorial Institute was conducted under USAEC contract AT(45-1)-1830. The efforts of the staff members of the Reactor Materials Branch at NRL and of the Irradiation Damage Effects Unit at Battelle in support of this study are acknowledged with appreciation. Special thanks are accorded to C.H. Hogg and K.L. Rasmussen of the counting room staff of Idaho Nuclear Corporation, Materials Testing Reactor, for their efforts in counting and analyzing all of the neutron-flux monitoring foils used for this study. The authors wish to note that studies of this kind cannot be accomplished in a short time, and thus, they are very appreciative of the long-term support that has been given by the sponsors for this purpose.

## REFERENCES

1. Harries, D.R., Barton, P.J., and Wright, S.B., "Effects of Neutron Spectrum and Dose Rate on Radiation Hardening and Embrittlement in Steels," Symposium on Radiation Effects on Metals and Neutron Dosimetry, STP 341, Am Soc. Testing Materials (1963)
2. Shure, K., "Radiation Damage Exposure and Embrittlement of Reactor Pressure Vessels," WAPD-TM-471, Bettis Atomic Power Laboratory, Nov. 1964
3. Rossin, A.D., Nucl. Structural Eng. 1 (1965) 76
4. Dahl, R.E., and Yoshikawa, H.H., "Neutron-Exposure Correlation For Radiation-Damage Studies," Nucl. Sci. Eng. 21:312 (1965)
5. Rossin, A.D., "Reporting Neutron Exposure for Radiation Damage," in "Interaction of Radiation with Solids," Proc. Cairo Solid State Conference, Cairo, Egypt (Sept. 1966), New York:Plenum Press, 1967, p. 553
6. Sheely, W.F., Nucl. Sci. Eng. 29:165 (1967)
7. McElroy, W.N., Dahl, R.E., Jr., and Serpan, C.Z., Jr., "Damage Functions and Data Correlation," Nucl. Applications, (pending publication)
8. Dahl, R.E., Jr., Ulseth, J.A., and Busselman, G.J., Battelle-Northwest Laboratory, private communications to C.Z. Serpan, Jr., Naval Research Laboratory, Washington, D.C., 1968
9. Little, W.W., Jr., and Hardie, R.W., "2DB Users Manual," BNWL-831, Battelle-Northwest Laboratory, Aug. 1968
10. Duane, B.H., "Neutron and Photon Transport Plane-Cylinder-Sphere (GE-ANPD) Program S Variational Optimum Formulation," XDC-9-118, General Electric Company, Cincinnati, 1959
11. Bengston, J., and others, "2DXY Two-Dimensional, Cartesian Coordinate Sn Transport Calculation," USAEC Report AGNTM-392, June 1961
12. Helm, J.W., "High-Temperature Graphite Irradiations: 800 to 1200 Degrees C: Interim Report No. 1," BNWL-112, Battelle-Northwest Laboratory, Sept. 1965
13. Serpan, C.Z., Jr., and Hawthorne, J.R., Trans. Am Soc. Mech. Engrs. 89D4:897 (Dec. 1967)
14. Serpan, C.Z., Jr., and Steele, L.E., "Damaging Neutron Exposure Criteria for Evaluating the Embrittlement of Reactor Pressure Vessel Steels in Different Neutron Spectra," Symposium on the Effects of Radiation on Structural Metals, STP 426, Am Soc. Testing Materials, Pa., 1967, p. 594
15. McElroy, W.N., and others, "A Computer-Automated Iterative Method for Neutron Flux Spectra Determination by Foil Activation," AWFL-TR-67-41 Vols. I, II, III, and IV, Air Force Weapons Laboratory, Albuquerque, N.M., Sept. 1967
16. Landerman, E., "Surveillance Tests on Structural Materials in Nuclear Reactors," Symposium on Radiation Effects on Metals and Neutron Dosimetry, STP 341, Am Soc. Testing Materials, Philadelphia, Pa., p. 233, 1963

17. Serpan, C.Z., Jr., and Watson, H.E., "Notch Ductility, Tensile and Neutron Spectrum Analyses of the PM-2A Reactor Pressure Vessel," Symposium on the Effects of Radiation on Structural Metals, STP 457, Am Soc. Testing Materials, Philadelphia, Pa. (pending publication) 1969



## DOCUMENT CONTROL DATA - R &amp; D

(Security classification of title, body of abstract and indexing annotation must be entered when the overall report is classified)

|  |                              |   |  |
|--|------------------------------|---|--|
| 1. ORIGINATING ACTIVITY (Corporate author)<br>Naval Research Laboratory<br>Washington, D.C., 20390   |                              | 2a. REPORT SECURITY CLASSIFICATION<br>Unclassified  |  |
|  |                              | 2b. GROUP   |  |
| 3. REPORT TITLE<br>DAMAGE-FUNCTION ANALYSIS OF NEUTRON-ENERGY AND SPECTRUM EFFECTS UPON THE RADIATION EMBRITTLEMENT OF STEELS  |                              |   |  |
| 4. DESCRIPTIVE NOTES (Type of report and inclusive dates)<br>An interim status report; work is continuing.   |                              |   |  |
| 5. AUTHOR(S) (First name, middle initial, last name)<br>Serpan, C.Z., Jr.<br>McElroy, W.N.   |                              |   |  |
| 6. REPORT DATE<br>July 25, 1969  | 7a. TOTAL NO. OF PAGES<br>20 | 7b. NO. OF REFS<br>17   |  |
| 8a. CONTRACT OR GRANT NO.<br>NRL Problem M01-14  |                              | 9a. ORIGINATOR'S REPORT NUMBER(S)<br>NRL Report 6925  |  |
| b. PROJECT NO.<br>RR007-11-41-5409   |                              |   |  |
| c. USA-ERG-11-69   |                              |   |  |
| d. AEC-AT(49-5)-2110   |                              | 9b. OTHER REPORT NO(S) (Any other numbers that may be assigned this report)   |  |
| 10. DISTRIBUTION STATEMENT<br>This document has been approved for public release and sale; its distribution is unlimited.  |                              |   |  |
| 11. SUPPLEMENTARY NOTES<br>U.S. Atomic Energy Commission, DRDT,<br>Washington, D.C., 20545   |                              | 12. SPONSORING MILITARY ACTIVITY Department of the Navy (Office of Naval Research) Washington, D.C., 20360, U.S. Army Engineer Research Group, Ft. Belvoir, Va. |  |
| 13. ABSTRACT<br>Critical evaluations of irradiation effects data for steels exposed in different reactor environments depend upon fluence measurements that reflect the neutron population and the corresponding influence of damage mechanisms inherent to those neutron energy spectra. For the present research investigation, theoretical models describing neutron damage in reactors were adjusted with data on mechanical property changes of A302-B steel irradiated at <math>450^{\circ}\text{F}</math> (<math>232^{\circ}\text{C}</math>). As described previously, this procedure yielded a damage function that more properly accounts for the energy dependence of damage.<br><br>The present investigation was centered on a new comprehensive experiment which yielded wide variations in spectra and in corresponding measurements of neutron embrittlement. The experiment and the resultant data have validated the damage function. An important new part of the damage function analysis technique provides the percent contributions of neutrons of all energy levels to the embrittlement process. Values of the damage function, averaged for a typical reactor physics spectral calculation group structure, are presented with suitable descriptions of their applications to a wide variety of spectra.<br><br>One major conclusion reached in this study is that detailed as well as accurate neutron dosimetry measurements of fast and thermal fluxes, corrected to reactor operating temperatures, are necessary if good correlations among irradiation-effects data are to be obtained. This requirement applies to both experimental irradiations and irradiations at reactor component surveillance locations. The study has shown<br>(continues) |                              |   |  |

| 14. KEY WORDS   | LINK A |    | LINK B |    | LINK C |    |
|---|--------|----|--------|----|--------|----|
|   | ROLE   | WT | ROLE   | WT | ROLE   | WT |
| Reactors<br>Neutron Flux<br>Neutron Fluence<br>Neutron Spectrum<br>Thermal Neutrons<br>Fast Neutrons<br>Neutron Embrittlement<br>Damage Model<br>Damage Function<br>Pressure Vessel Steel |        |    |        |    |        |    |

ABSTRACT (continued)

further that an independently derived damage function for irradiation of structural steels such as A302-B at <450°F (232°C) is realistic and can be applied to new experimental data conforming to those conditions. The contributions of thermal and low-energy neutrons to the embrittlement process in low-alloy steel are shown to be of major importance to the interpretation of radiation-effects data.